Transactions of the Materials Research Society of Japan 30[3] 675-678 (2005)

Bilayer Structure Fluctuation of Amphiphilic Compounds during Self-Assemble Polymerization in Two Dimensional Anisotropic Field

T. Yamada[1], T. Yoshii[1], N. Ozawa[1], Y. Kawabata[2], T. Kato[2], H. Yoshida[1,3]

1: Graduate School of Engineering, Tokyo Metropolitan University,
1-1 Minamiosawa, Hachioji, Tokyo 192-0397, Japan
Fax: +81-426-77-2821, e-mail: yamada-takesi@c.metro-u.ac.jp
2: Graduate School of Science, Tokyo Metropolitan University1-1 Minamiosawa, Hachioji, Tokyo 192-0397, Japan
Fax: +81-426-77-2525
3: CREST-JST, 4-1-8, Honmachi, Kawaguchi 332-0012, Japan

The amphiphilic monomer consisting of trialkyl ammonium salts and styrene units formed the self assemble bilayer structure. By irradiation of X-ray during the phase transition from the crystalline state to the smectic phase, the bilayer structure of monomer was fixed in its polymeric compound by "self assemble polymerization". The phase transition behavior and structural changes of model compound, which had ethyl benzene units instead of styrene unit, were investigated by the simultaneous DSC-SAXS measurement. The structural fluctuation change of alkyl chains, hydrophilic part and ethyl benzene unit were evaluated by the SAXS profile fitting. The disordering of alkyl chains occurred at the beginning of phase transition, and the ordering of ethyl benzene unit occurred during the phase transition. The mechanism of "self assemble polymerization" was proposed that the vinyl groups belonging to the closed bilayers aligned in the same two dimensional field during the phase transition and the "self assemble polymerization" occurred.

Key Words: phase transition / self-assemble structure / anisotropic field / structure fluctuation/ amphiphic monomer

I. INTRODUCTION

Controlling high-order structure of polymers has been paid many attentions in order to develop advanced functional materials. Various processing methods are applied to polymers under the stretching force, pressure, magnetic and electric fields to control high-order structure of polymers. However, it is difficult to control the long range order of polymers because the entropy loss due to conformational ordering is higher than the enthalpy gain due to orientational ordering of polymer chains. From thermodynamic viewpoint, to control long range order of low molecular weight materials is much easy than polymers. Thus, several trials to fix the order structure of monomers into polymers by specified polymerization techniques, such as photo-polymerization of monomer single crystal [1], as-polymerized crystallization [2] and polymerization in vesicles [3, 4]. The needle like single crystal of poly(oximethylene) is obtained upon cationic polymerization [2], and the monolayer polymer is reported by polymerization in vesicles [3]. Although amphiphilic monomers are polymerized in the bilayer vesicles, the order structure of bilayer is vanished by polymerization [5, 6] and the size of obtained polymer by these methods is below mm, it is too small to use as a functional engineering materials.

Recently, we have proposed the "self-asseble polymerization" in which the self-assemble structure of amphiphilic monomer on various substrates was fixed into the polymers by irradiating low energy electron beam or X-ray [7, 8]. The optical transparent polymer films were obtained by the "self-assemble polymerization" of amphiphilic monomer consisting of trialkyl ammonium [8] or trialkyl phosponium salts [9]. The obtained polymers were composed of the stacked bilayer structure, which was formed by amphiphilic monomers on the substrates. That is to say, the polymers obtained by the "self-assemble polymerization" has the anisotropic structure in which the ordered bilayers are stacked parallel to the polymer surface and low ordered alignments exist in the direction perpendicular to the polymer surface [10]. During the "self-assemble polymerization" of amphiphilic monomers, vinyl groups aligned in two dimensional anisotropic interface between bilayers. The distance and ordering between vinyl groups in the interface have the important role of "self-assemble polymerization".

In this study, the structural changes of bilayers during the "self-assemble polymerization" were investigated by the profile fitting of small angle X-ray scattering (SAXS) profiles in order to analyze the mechanism of "self-assemble polymerization" of amphiphilic monomers. However, the polymerization of amphiphilic monomer occurred easily by irradiating X-ray. Therefore, the model compound having ethyl groups instead of vinyl groups was synthesized and used for the SAXS measurement in this study.

II. EXPERIMENTS

Amphiphilic monomer ($M_2$18, scheme 1) was synthesized from N, N,-di-n-octadecylmethylamine and p-chlorometylstylene in di-chloromethane solution for 48 hrs at room temperature. Model compound ($E_2$18, scheme 2) was synthesized from N, N,-di-n-octadecylmethylamine and chloromethyl-4-ethyl-benzene in dichloromethane solution for 48 hrs at room temperature. The obtained $M_2$18 and $E_2$18 were purified by a column chromatography and re-crystallization, and were identified by FAB-MASS and ^{1}H-NMR.

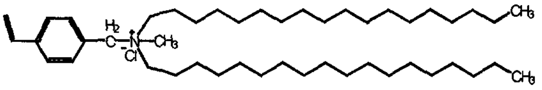

Scheme 1

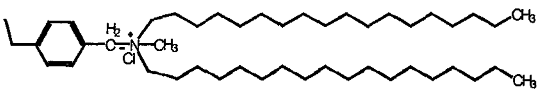

Scheme 2

Differential scanning calorimetry (DSC) measurements were performed by DSC 5200 (SEIKO Instruments Inc.) equipped with cooling control apparatus in the temperature range between -20 and 110 °C. Scanning rate was 1 K min^{-1} in a flowing nitrogen atmosphere (50 ml min^{-1}). Samples weight for DSC measurement was about 3 mg.

Simultaneous DSC and small angle X-ray scattering measurement (DSC-SAXS) were performed by a synchrotron radiation X-ray facility of the 2.5-GeV storage ring at BL-10C in Photon Factory, High Energy Accelerator Research Organization (Tsukuba, Japan). The simultaneous DSC instrument [11] was setting on SAXS optics, and the monochromatic synchrotron radiation X-ray by double Si crystals (the wavelength of X-ray was 0.1488 nm) was used for DSC-SAXS measurement. The distance between sample and one-dimensional position sensitive proportional photon counter (PSPC) was 560 mm, which covered $0.8 < q = 4\pi \sin\theta / \lambda < 5$ nm^{-1}, where θ and λ were a half of diffraction angle and X-ray wavelength, respectively. Scanning rate of DSC and time resolution of XRD were 5 K min^{-1} and 12 sec., the temperature resolution of one SAXS profile was 1 K [12]. Samples weight for DSC-SAXS measurement was about 10 mg.

III. RESULT AND DISCUSSION

As both samples decomposed at temperature above 120 °C, the solution grown crystals of $M_2$18 and $E_2$18 were heated up to 110 °C (1st heating) and cooled at 1 K min^{-1} to -20 °C. During cooling from 110 to -20 °C, both samples crystallized around 30 °C, the melt crystallized samples were heated again from -20 to 110 °C (2nd heating). DSC 2nd heating curves of $M_2$18 and $E_2$18 were shown in Fig. 1.

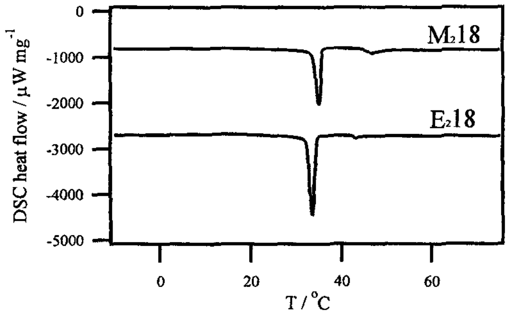

Fig.1: DSC heating curves of $M_2$18 and $E_2$18 obtained at 1 Kmin^{-1}. Both samples were prepared by cooling at 1 Kmin^{-1} from 110 to – 20 °C.

Two endothermic peaks were observed for both samples, these endothermic peaks were also observed at similar temperature during 1st heating. From DSC-SAXS measurement described below, the endothermic peak at 30 °C corresponded to the transition from crystal to smectic state, because the diffraction peak from the smectic layer remained in the temperature range above this transition to 110 °C. The origin of small endothermic peak at around 40 °C was not clear in detail at present, however, this transition related to the transition between the smectic phases. The transition from crystal to smectic state was observed at 33.7 and 32.3 °C for $M_2$18 and $E_2$18, respectively. The transition entropy of $M_2$18 and $E_2$18 was 115.3 and 124.7 JK^{-1} mol^{-1}, respectively. The transition entropy difference between both samples was less than the entropy due to the conformational freedom of one carbon-carbon linkage ($\Delta S = R\ln 3 = 9.1$ JK^{-1} mol^{-1}). The entropy difference was a result of freedom difference between vinyl group of $M_2$18 and ethyl group of $E_2$18. These results suggested that the phase transition behavior of $M_2$18 and $E_2$18 were essentially the same. This indicated that $M_2$18 and

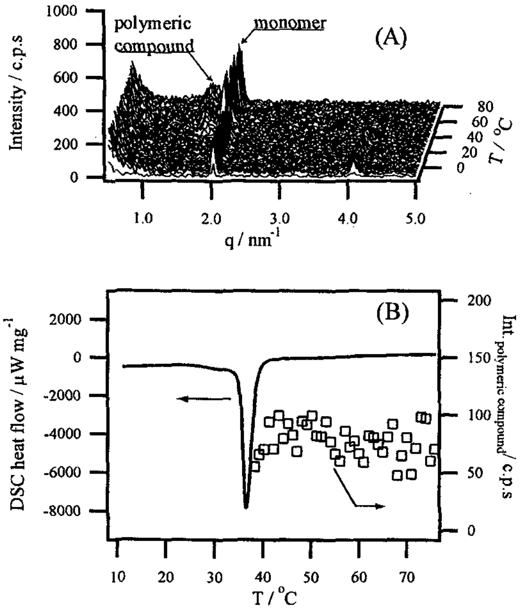

Fig.2: Stacked SAXS profiles of $M_2$18 observed during heating by the simultaneous DSC-SAXS method at 5 Kmin^{-1} (A), and the intensity change of diffraction peak corresponding to (001) plane of polymeric compound overlapped with DSC heating curve (B).

$E_2$18 had the same phase transition.

Stacked SAXS profiles of $M_2$18 obtained by DSC-SAXS on heating were shown in Fig. 2 (A). Two diffraction peaks were observed at 2.05 and 4.1 nm^{-1} at room temperature, which were assigned to (001) and (002) plane of lamellar structure, respectively. The distance of $(001)_L$ plane was 2.9nm, which was 20 % longer than the $M_2$18 assuming all trans conformation. N, N, -di-n-octadecyl methylamines form bilayer structure with evaluating the electron density correlation function form SAXS profile [16], $M_2$18 formed bilayer structure. From the molecular length of $M_2$18 evaluated by the molecular mechanical calculation, $M_2$18 molecules tilted about 32° from the substrate plane in the bilayer. The new broad diffraction peaks were observed at 1.7 nm^{-1} at temperatures above 35 °C. These peaks correspond to a lamellar structure of the polymer, because the insoluble fraction in methanol, which was good solvent for $M_2$18, was obtained from the samples after DSC-SAXS measurement. As the peak width and the intensity of $(001)_L$ and $(002)_L$ of the obtained polymer were broader and weaker than the monomer, the order of lamellar structure in polymer obtained by the "self-assemble polymerization" was lower than the self-assemble lamellar structure of monomer. At the temperature range above 35 °C, both $(001)_L$ peaks of $M_2$18 and polymeric compound were observed. The intensity change of $(001)_L$ of the polymeric compound was plotted with DSC heating curve in Fig. 2 (B). The $(001)_L$ peak of polymer appeared immediately after the transition peak, and the peak intensity increased and leveled off with increasing temperature.

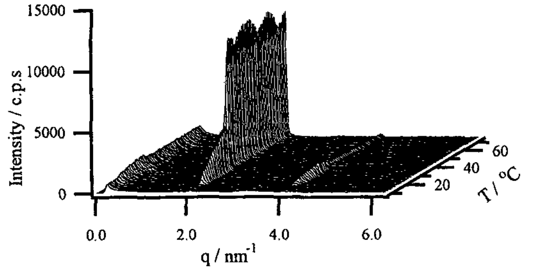

Fig.3: Stacked SAXS pforiles of $E_2$18 obtained by the simultaneous DSX-SAXS measurment at 5 Kmin^{-1}.

Fig. 3 shows the stacked SAXS profiles of $E_2$18 obtained by the simultaneous DSX-SAXS measurement during heating. Two diffraction peaks due to $(001)_L$ and $(002)_L$ of $E_2$18 are observed at the same q range with $M_2$18. No peaks corresponding to polymer structure were observed at temperature above 35 °C. The SAXS profiles obtained by DSC-SAXS were analyzed by the profile fitting of multilamellar structure model proposed by Lemmich et al [13]. As this model evaluate the profiles without decoupling the structure and the form factors based on the paracrystalline theory [14], the model is suitable for analyzing SAXS profiles upon phase transition in which the form factor changes.

Within this model, the bilayer structure of $E_2$18 was separated to alky chain part (AL), hydrophilic part including both ammonium and chloride ions (H) and ethyl benzene unit (EB) corresponding to polymerization unit. The scattering function was given as follows.

$$I(q) = \frac{\Gamma}{q^4}[i_B(q) + \frac{1}{N} i_c(q)] \tag{1}$$

$$i_B(q) = \mathrm{Re}[\frac{(1-F_{EB})(1-F_H^2 F_{AL})}{(1-F_D)} + \frac{(b_r-1)^2(1-F_{AL})(1-F_H^2 F_{EB})}{(1-F_D)}] \tag{2}$$

$$i_c(q) = \mathrm{Re}[F_{EB}(1-F_D^N)\left\{\frac{(1-F_{EB}F_{AL})}{(1-F_D)} + \frac{(b_r-1)F_{EB}(1-F_L)}{(1-F_D)}\right\}^2] \tag{3}$$

$$F_v(q) = \exp(-iqd_v - (1/2)q^2\sigma_v^2) \quad (v = H, AL, EB) \tag{4}$$

$$F_D(q) = F_H^2 F_{AL} F_{EB} \tag{5}$$

$$b_r = \frac{(b_{AL} - b_{EB})}{(b_H - b_{EB})} \tag{6}$$

The thickness of the layers is assumed to fluctuate independently according to Gaussian distribution with mean values d_{AL}, d_H and d_{EB} and corresponding standard deviations σ_{AL}, σ_H and σ_{EB}. The electron density of each parts were indicated by b_v (v = AL, H, EB). N and G indicated the number of stacked layers and the normalization constant, respectively.

The experimental SAXS profile at room temperature and the fitting result calculated by eq. (1) were shown in Fig. 4. The σ_H vale was fixed to 0 nm during calculation because the hydrophilic part was thin and its fluctuation was small. The good agreement was obtained between the experimental SAXS profile and the calculated results in the q range between 1.5 and 4.5 nm^{-1}. The obtained fitting parameters of the best result were d_H = 0.19139 nm, d_{EB} = 1.0902 nm, d_{AL}=1.588 nm, σ_{EB} = 0.13728 nm, σ_{AL} = 0.094087 nm, b_r = 0.11362, N = 410.34, G = 2.8358. The SAXS profiles obtained at various temperatures were analyzed by the profile fitting.

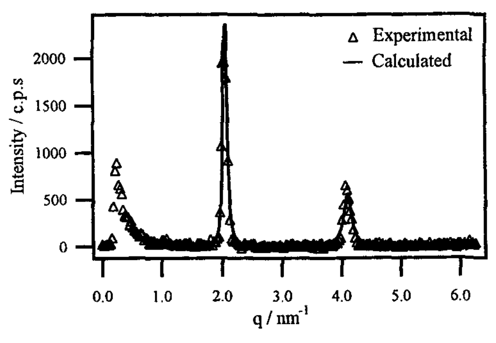

Fig.4: Experimental SAXS profile (triangle) of $E_2$18 observed at room temperature by the simultaneous DSC-SAXS method and the profile fitting results (solid line).

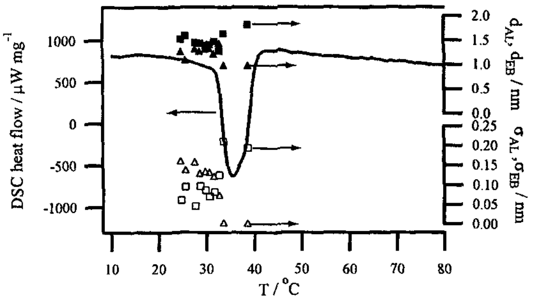

Fig.5: Distance changes of ethyl benzene unit (filled triangle) and alkyl chains (filled square) and structure fluctuation changes of ethyl benzene unit (triangle) and alkyl chains (square) evaluated by the SAXS profile fitting of $E_2$18 observed by the simultaneous DSC-SAXS method overlapped with DSC heating curve.

The distance and structure fluctuations of alkyl chain (d_{AL}, σ_{AL}) and ethyl benzene parts (d_{EB}, σ_{EB}) obtained by the profile fitting of SAXS profiles at various temperatures were plotted with DSC curve obtained by DSC-SAXS in Fig.5. The d_{EB} decreased about 0.3 nm and σ_{EB} approached to 0 during the phase transition. On the other hand, d_{AL} increased about 0.3 nm and σ_{AL} almost increased to constant value during the phase transition. The large values of σ_{EB} and σ_{AL} indicate the disordering of each part, the decrease of σ_{EB} at the phase transition suggests that the ordering of ethyl benzene part occurred with the melting. However, above 40 °C the fitting became difficult because the SAXS intensity decreased extremely after the phase transition.

The results shown in Fig.5 suggested that the following structural changes occurred during the phase transition. Vinyl groups in styrene units of amphiphilic monomers aligned in each bilayers in the crystalline state as shown in Fig. 6 (A), which was supported by the electron diffraction of bilayer [15]. The distance between vinyl groups in the same layer is about 0.2 nm, which is too far to react between vinyl groups. At the beginning of phase transition, the disordering of long alkyl chains occurred because the ordering of alkyl chains were supported by weak van der Waals interactions, and the molecular motion of long alkyl chains increased σ_{AL}. As d_{EB} values decreased during the phase transition, vinyl groups existed in the upper and lower bilayers aligned in the same layer as shown in Fig.6 (B) with increasing the molecular motion of alkyl chains. These coagulations of vinyl groups increased the order of interface and σ_{EB} value decreased. The distance between vinyl groups shown in Fig. 6 (B) is estimated about 0.1 nm, which is sufficiently close each other to occur polymerization. The "self-assemble polymerization" occurred in two dimensional anisotropic field caused by the fluctuation ordering of bilayers accompanying with the phase transition.

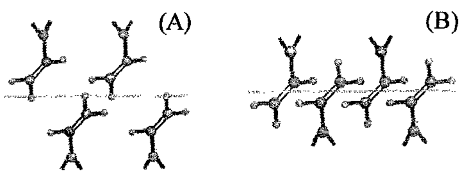

before phase transition

initial stage of phase transition

Fig.6: Schematic image of the ordering change of the polymerization unit during phase transition.

IV. Conclusions

The "self-assemble polymerization" of trialkyl ammonium salt type amphiphilic monomer $M_2$18 occurred during the phase transition from the crystal to the smectic phase at 33 °C. With evaluating the distance and the structure fluctuation, the polymerization part existed in the upper and lower bilayers aligned in the same layer the ordering of the polymerization part occurred during the phase transition. The mechanism of "self-assemble polymerization" of amphiphilic monomer was proposed.

Reference

[1] R. Mayer, R. Wagner, J. Fabian, *Z. Naturforsch*, **24B**, 24, (1969)
[2] M. Iguchi, Brit. *Polymer J.*, **5**, 195, (1973)
[3] M. Hatada, M. Nishii, K. Hirota, *J.colloid interface Sci.*, **45**, 502, (1973)
[4] R. Elbert, A. Lashewsky, H. Ringsdorf, *J. Am. Chem. Soc.*, **107**, 4134, (1985)
[5] J. Leaver, A. Alonso, A. Durrani, D. Chaoman, *Biochim. Biophys. Acta*, **732**, 210, (1983)
[6] T. Kunitake, N. Nakashima, M. Kunitake, *Macromolecules*, **22**, 3544, (1989)
[7] T. Yoshii, H. Yoshida, T. Kawai, *2nd Int. Symp. New Frontiers Thermal Study Materials*, **122**, (2001)
[8] T. Yoshii, N. Ozawa, T. Kawai, T. Ito, H. Yoshida, *Polym. Preprints Japan*, **51**, 428, (2002)
[9] T. Yamada, T. Tanaka, A. Shiina, H. Yoshida, *Polym. Preprints Japan*, **53**, 853, (2004)
[10] H. Yoshida, T. Kato, S. Komura, M. Fujii, Y. Kawabata, T. Takei, K. Sato, *Memoirs Grad. Shool Eng. Tokyo Metropolitan University*, **54**, 1, (2004)
[11] H. Yoshida, R. Kinoshita, Y. Teramoto, *Thermo chimica Acta*, **264**, 173-183, (1995)
[12] H. Yoshida, *Thermochim. Acta*, **267**, 239, (1995)
[13] J. Lemmich, K. Mortensen, J. H. Ipsen, T. Honger, R. Bauer, O. G. Mouritsen, *Phys. Rev. E*, **53**, 5169-5180, (1996)
[14] R. Hosemann, S. N. Bagchi, "Direct Analysis of Diffraction by Matter", p. 216, North-Holland, Amsterdam, (1962)
[15] H. Yoshida, T. Yoshida, T. Yamada, *IUMRS-ICAM 2003*, **Symp. A-2**, p. 14, (2003)
[16] T. Yui H. Yoshida, H. Tachibana, D. A. Tryk, H. Inoue, *Langmuir*, **18**, 891-896, (2002)

(Received December 23, 2004; Accepted April 21, 2005)